Model-Simulated Northern Winter Cyclone and Anticyclone Activity under a Greenhouse Warming Scenario

YI ZHANG

Program for Climate Model Diagnosis and Intercomparison, Lawrence Livermore National Laboratory, Livermore, California

WEI-CHYUNG WANG

Atmospheric Science Research Center, State University of New York at Albany, Albany, New York

(Manuscript received 19 April 1996, in final form 4 November 1996)

ABSTRACT

Two 100-yr equilibrium simulations from the NCAR Community Climate Model coupled to a nondynamic slab ocean are used to investigate the activity of northern winter extratropical cyclones and anticyclones under a greenhouse warming scenario. The first simulation uses the 1990 observed CO_2, CH_4, N_2O, CFC-11, and CFC-12 concentrations, and the second adopts the year 2050 concentrations according to the Intergovernmental Panel on Climate Change business-as-usual scenario. Variables that describe the characteristic properties of the cyclone-scale eddies, such as surface cyclone and anticyclone frequency and the bandpassed root-mean-square of 500-hPa geopotential height, along with the Eady growth rate maximum, form a framework for the analysis of the cyclone and anticyclone activity.

Objective criteria are developed for identifying cyclone and anticyclone occurrences based on the 1000-hPa geopotential height and vorticity fields and tested using ECMWF analyses. The potential changes of the eddy activity under the greenhouse warming climate are then examined. Results indicate that the activity of cyclone-scale eddies decreases under the greenhouse warming scenario. This is not only reflected in the surface cyclone and anticyclone frequency and in the bandpassed rms of 500-hPa geopotential height, but is also discerned from the Eady growth rate maximum. Based on the analysis, three different physical mechanisms responsible for the decreased eddy activity are discussed: 1) a decrease of the extratropical meridional temperature gradient from the surface to the midtroposphere, 2) a reduction in the land–sea thermal contrast in the east coastal regions of the Asian and North American continents, and 3) an increase in the eddy meridional latent heat fluxes. Uncertainties in the results related to the limitations of the model and the model equilibrium simulations are discussed.

1. Introduction

The passage of extratropical cyclones and anticyclones is closely linked to the day-to-day weather changes and local climate in the midlatitudes. These cyclone-scale eddies play an important role in transporting heat, momentum, and moisture in the extratropical regions and are an indispensable part of the general circulation of the atmosphere (Newton 1969). Study of the long-term variation of extratropical cyclone and anticyclone activity is thus essential for the understanding of extratropical climate change.

Although extensive research has greatly improved our understanding of nearly all aspects of extratropical cyclones and anticyclones (Newton and Holopainen 1990), our knowledge of the long-term climatology of cyclones and anticyclones is still very limited. The most often cited works on this subject are still those of Petterssen (1956) and Klein (1958). In addition, almost all of the studies in this area to date have been devoted to documenting the observed long-term variations of cyclone and anticyclone frequency and intensity, although the physical mechanisms that affect the variations of the long-term cyclone-scale eddy activity are not well understood. For example, the cause of the drastic decrease in cyclone and anticyclone frequency from the 1950s to the 1970s in North America as documented by Zishka and Smith (1980) and Whittaker and Horn (1981) is still a mystery.

The long-term variation in cyclone and anticyclone activity is known to be important to the general circulation of the atmosphere and is related to the global radiation balance because the heat transported by these eddies dominates the total atmospheric energy transport in the midlatitudes (Holopainen 1965). The global radiation balance can be disturbed by many factors, typically the increases in atmospheric greenhouse gas concentration and aerosol loadings. In this study, the response of cyclone and anticyclone activity to a global radiative perturbation will be examined by investigating eddy activity under the greenhouse warming scenario. To achieve this goal, relevant interacting physical processes in the climate system have to be considered. General circulation models (GCMs), which have long been recognized as the best available means for considering simultaneously the wide range of interacting physical processes that characterize the climate system, will be used in this study.

Corresponding author address: Dr. Yi Zhang, Program for Climate Model Diagnosis and Intercomparison, Lawrence Livermore National Laboratory, Livermore, CA 94550.
E-mail: zhang@pcmdi.LLNL.gov

TABLE 1. GCM-simulated changes of global and annual mean surface air temperatures Ts(K), precipitation P (mm day^{-1}), cloud cover C (%) and column water vapor Q (mm). (After Wang et al. 1992.)

Case	Ts	dTs	P	dP	C	dC	Q	dQ
1990	288.9	—	3.39	—	46.0	—	25.5	—
2050	292.8	3.88	3.64	0.25	44.6	−1.4	32.4	6.9

There have been several GCM studies related to cyclone and anticyclone activity under increased CO_2 conditions. Bates and Meehl (1985) indicated that the activity of northern winter baroclinic eddies and persistent anticyclones decreased with increased CO_2 in a version of National Center for Atmospheric Research (NCAR) Community Climate Model (CCM). Konig et al. (1993), based on analysis of model-simulated Northern Hemisphere surface cyclone frequency, suggested that there is no significant difference in cyclone frequency between the greenhouse warming and normal climate conditions. More recently, Hall et al. (1994) showed that the eddy kinetic energy near the storm tracks increased by approximately 10% in a 2 $\times$ CO_2 simulation of a high-resolution GCM; Lambert (1995) indicated, using the Canadian Climate Centre model, that the total number of Northern Hemisphere winter cyclones decreased and the frequency of intense cyclones increased under 2 $\times$ CO_2 conditions.

All of these studies have addressed the important issue of the possible changes in the activity of cyclone-scale eddies under the greenhouse warming condition. Differences in the conclusions of the studies may stem from their using different methods in approaching the problem and the model dependence of the results. These studies could also have adopted a more complete set of variables. For example, the only quantity used in Konig et al. (1993) was cyclone frequency at 1000 hPa; Lambert (1995) also focused on the surface cyclone frequency and intensity. Because the extratropical cyclones and anticyclones are baroclinic disturbances and extend from the surface to the middle and upper troposphere, a better approach is to study both the surface and the 500-hPa fields so that these eddies can be examined three-dimensionally. More importantly, none of the studies has adequately addressed the physical mechanisms that caused the changes in cyclone and anticyclone activity under the warming climate.

In order to better understand the cyclone and anticyclone activity under the greenhouse warming scenario, we will approach this problem more comprehensively than Lambert (1995), Konig et al. (1993), and others. Cyclone-scale eddy activity will be examined by using both the surface and 500-hPa quantities, as well as a quantity that relates to the basic flow baroclinicity. In addition, we will emphasize physical mechanisms that cause changes in cyclone and anticyclone activity under the warming scenario.

Historically, cyclones have been the focus of most studies since they are often associated with precipitation and stormy weather. It is actually more appropriate to include both cyclones and anticyclones, because the atmospheric variability and weather changes arise from the vorticity advection, which is related to the movement of both cyclones and anticyclones. Thus, the variables chosen for this study include 1) variables that describe the basic characteristics of both cyclones and anticyclones—that is, frequencies of surface cyclones and anticyclones and their geographic distribution—and the bandpassed (2.5–6 days) rms of 500-hPa geopotential height; and 2) the Eady growth rate maximum (or baroclinic parameter), a variable that represents the basic flow baroclinicity. These two groups of quantities will serve as a framework for examining the cyclones and anticyclones and for determining whether these eddies become more or less active under the greenhouse warming condition. Some of the variables will also be used to explain the physical mechanisms related to the changing eddy activity.

In section 2 we will briefly describe the model simulations and observational data. The design and testing of the objective criteria for identification of surface cyclones and anticyclones are discussed in section 3. The analysis of eddy activity under greenhouse warming conditions and the discussion of physical mechanisms are in section 4, and conclusions appear in section 5.

2. Model simulations and observational data

The model is based on version 1 of the NCAR Community Climate Model (CCM1), with the incorporation of the radiative effects of trace gases (CH_4, N_2O, CFC-11, and CFC-12). CCM1 is a spectral model with rhomboidal wavenumber 15 truncation. This truncation yields an effective grid resolution of 7.5° longitude and approximately 4.5° latitude. The model has 12 sigma levels in the vertical using energy-conserving vertical finite differences. Realistic land–ocean distributions and topography are used with the seasonal cycle included, and both large-scale condensation and moist convective adjustments are included in the cloud prediction schemes of the model. A detailed description of CCM1 can be found in Williamson et al. (1987).

Two 100-yr equilibrium simulations were performed (Wang et al. 1992) by coupling CCM1 with a 50-m mixed-layer ocean model containing seasonal heat storage and flux convergence (Covey and Thompson 1989), the first with observed 1990 concentrations of CO_2 and trace gases, and the second with increased concentrations of CO_2 and trace gases at the level of the year 2050 under the business-as-usual scenario of the Intergovernmental Panel on Climate Change (Houghton et al. 1990). The total radiative forcing calculated by the increase of trace gas concentrations between 1990 and 2050 is 3.1 W m^{-2}, which corresponds to an increase in CO_2 alone from the 1990 level of 354 ppmv to 660 ppmv. Although the recently revised scenario for future trace gas concentrations (Houghton et al. 1995) differs from the business-as-usual scenario, we do not expect that the difference is too large to affect the findings of this study. The comparisons between the two

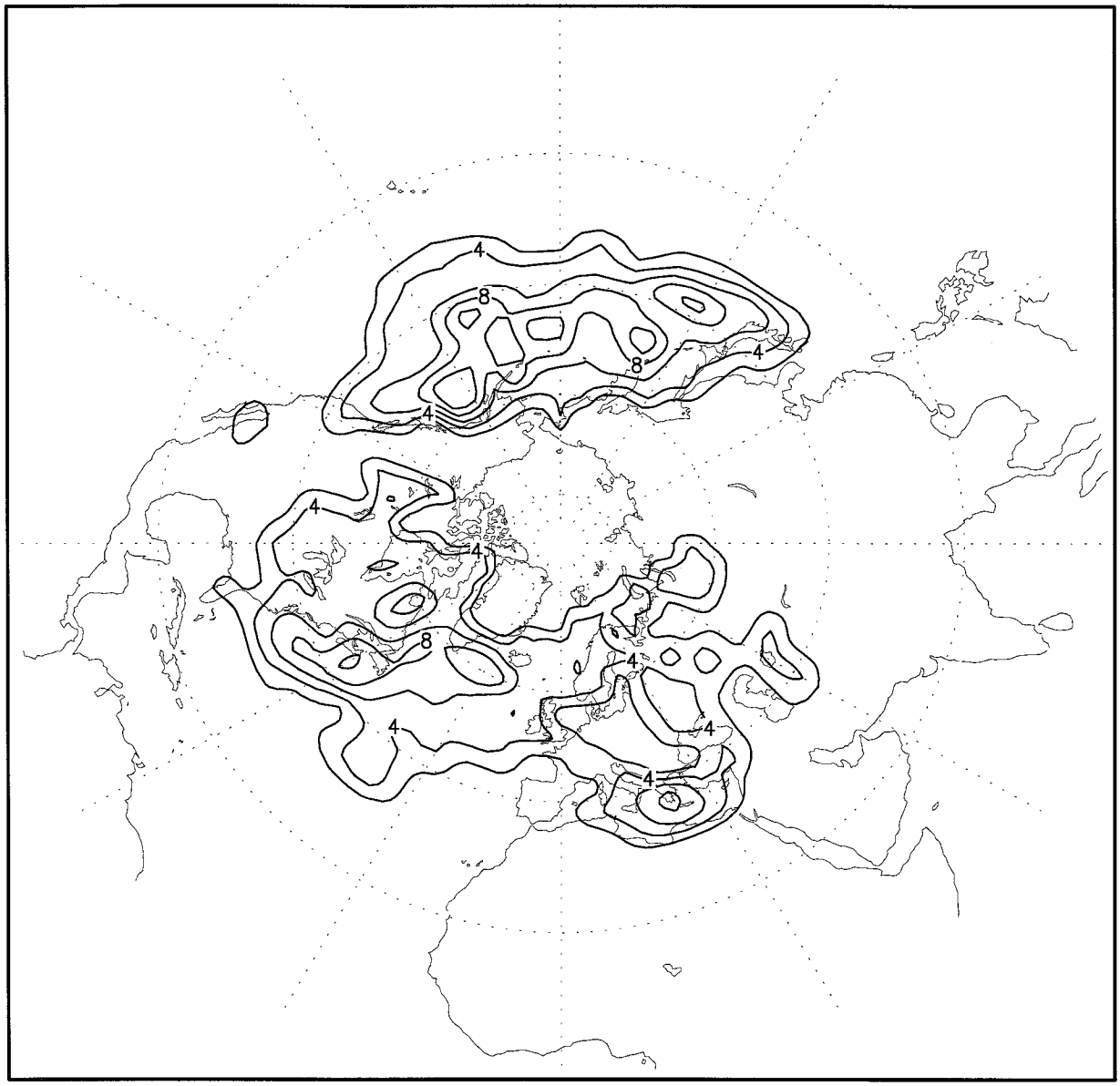

FIG. 1. (a) Winter seasonal averaged cyclone events from ECMWF global analyses (1979–88) identified through the cyclone searching criteria. Contour interval is 2. Units are the numbers of events per season. (b) Winter seasonal averaged percentage frequency of cyclone centers during 1899 to 1939 from Petterssen (1956). Units are the percentages of frequency (100 000 km^2)$^{-1}$.

simulations will provide the equilibrium climate changes due to projected increases of CO_2 and other trace gases between 1990 and 2050.

Global and annual mean changes of some important climate variables for the two cases are summarized in Table 1. The results indicate that increasing greenhouse gases can warm the global annual mean surface air temperature by 3.9°C. Consistent with this surface warming, the globally averaged cloud cover decreases, and the precipitation and moisture increase. These characteristics are similar to those of other GCM simulations of the greenhouse effect (Houghton et al. 1992). The inclusion of other trace gases in the current model yields a more realistic simulation of the surface and the upper-tropospheric temperature and humidity in the present climate than using CO_2 as a proxy (Wang et al. 1991). As will be discussed later, the variation of the meridional temperature gradient and water vapor are the two most important mechanisms that can affect the cyclone-scale eddy activity under the warming condition. Therefore, we believed that the improvement in the temperature and water vapor should lead to more realistic simulated changes of cyclone-scale eddy activity between the warming and control simulations.

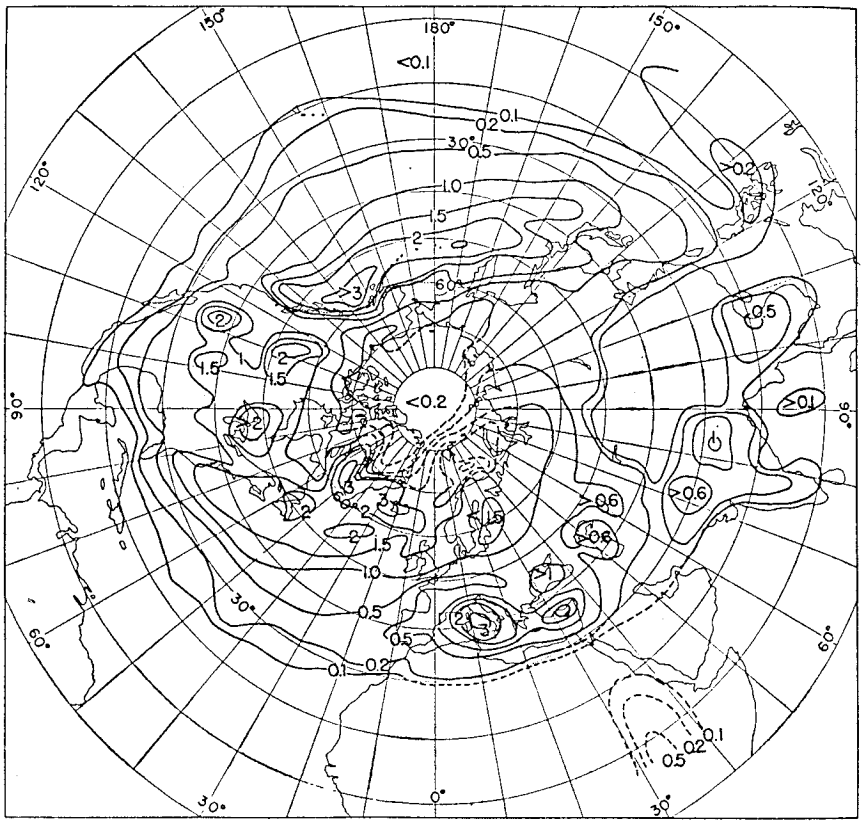

FIG. 1. (*Continued*)

Major characteristics of CCM1, such as circulation statistics, cloud radiative forcing, and sensitivity of climate simulations to horizontal resolution, have been examined (Kiehl and Williamson 1991). A complete documentation on CCM1-simulated circulation statistics is found in Williamson and Williamson (1987). These circulation statistics include some of the most characteristic fields of the transient eddies, such as bandpassed eddy heat and momentum fluxes, the rms of bandpassed 500-hPa geopotential height, etc. Most of these simulated quantities are in general agreement with observations. Because the current model is slightly different from the standard version of CCM1, we have performed a complete evaluation on the characteristics fields of transient eddies in the control simulation (Zhang 1995). The results, similar to those of Williamson and Williamson (1987), have indicated that the model has skill in reproducing most eddy-related quantities.

Observational data for testing the cyclone-searching criteria are from 10 yr (1979–88) of European Centre for Medium-Range Weather Forecasts (ECMWF) December–February (DJF) initialized analysis. For consistency between the horizontal resolution of the model and the observations, the R15 version of the ECMWF analyses will be used for the testing. All the analyses and figures to be shown are for the 10-yr northern winter (DJF) average unless otherwise specified. This decision was made mainly based on the length of the available observed data and the length of the model simulations. The 10-yr duration seems to be long enough to have fairly stable statistics of most variables, such as temperature, wind, and surface cyclone frequency. To be cautious, comparisons between 10- and 30-yr averaging were made on selected model simulated quantities. The comparisons indicate that the spans of 10 yr produce the same results as those of 30 yr. Ten yr of observational data and model output have been used to study extratropical eddy activity and storm tracks by other investigators as well (Hoskins and Valdes 1990; Trenberth 1991).

3. Criteria for identifying cyclones and anticyclones

A proper set of numerical criteria for identifying cyclones and anticyclones in the model is needed for this study. Considering the scale and characteristics of extratropical cyclones and anticyclones, the following criteria have been designed to identify cyclones and anticyclones in the extratropical regions (25° to 70°N).

1) Minimum (maximum) 1000-hPa geopotential height

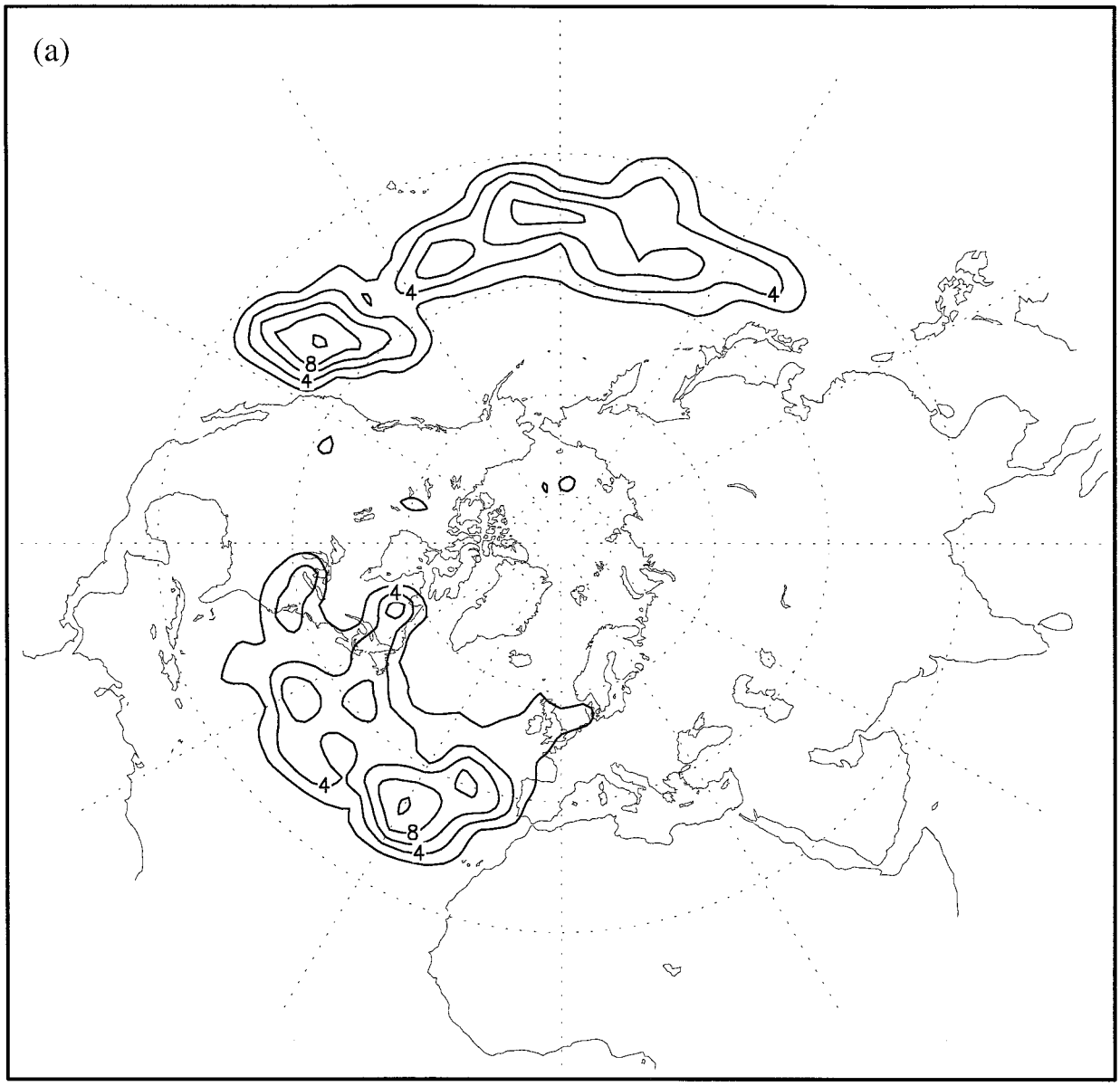

FIG. 2a. Same as in Fig. 1a except for anticyclones.

at the grid point relative to the eight surrounding points is required.

2) Identified cyclone (anticyclone) vorticity at the grid point must remain for at least 24 h.
3) Relative vorticity magnitude at 1000 hPa must exceed a critical value of 2.0×10^{-5} s^{-1} (or 1.0×10^{-5} s^{-1}).

Disturbances satisfying the above criteria are defined as cyclones (anticyclones). Multicounting of the same cyclone (anticyclone) at one grid point in adjacent time periods must be avoided because the criteria are applied to the data twice a day. To do this, we explicitly limit at most one cyclone or anticyclone at one grid point within 48 h. Due to the coarse resolution of the model, the representation of high terrain is quite crude. Computational biases arise in the vicinity of the Tibetan Plateau when the 1000-hPa fields are interpolated. Any points that are in the plateau or within two grid points of the plateau are excluded from the counting. These identification criteria, similar to those of Konig et al. (1993) and Lambert (1988), use the minimum 1000-hPa geopotential height as the quantity for initial identification. Constraints on the magnitude and duration of the 1000-hPa vorticity field are then applied for further identification.

Based on the above criteria, the cyclone events are counted for 10 yr (1979–88) from the ECMWF observational analyses (shown in Fig. 1a). Comparing the per-

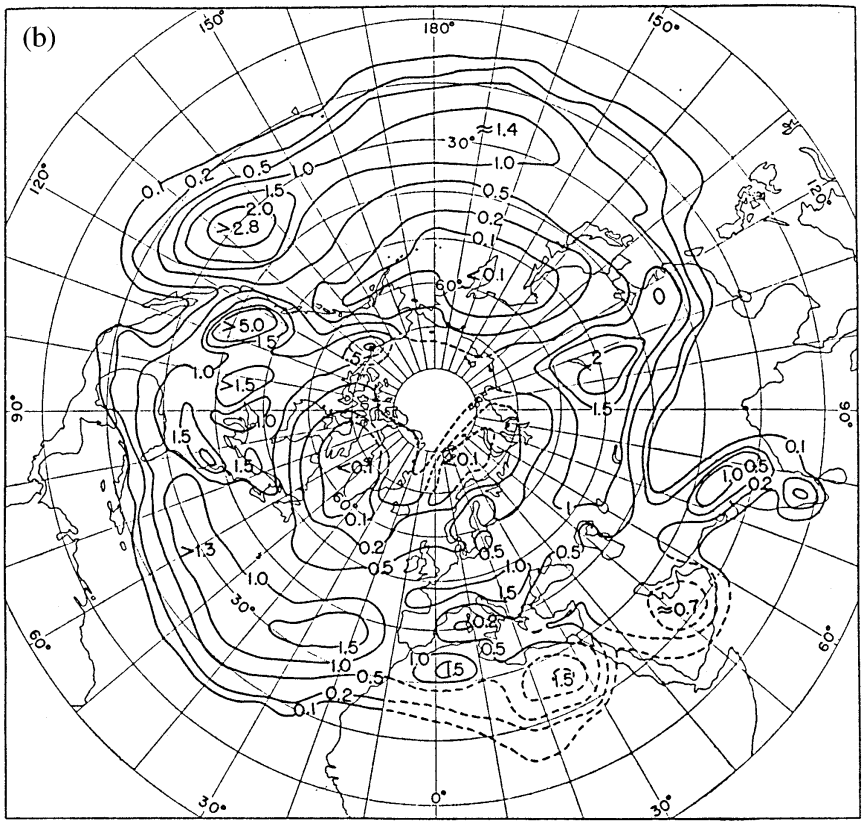

FIG. 2b. Same as in Fig. 1a except for anticyclones.

centage of frequency of cyclone centers from Petterssen (1956) in Fig. 1b, we find that the maximum cyclone frequency centers are remarkably close. The geographic locations of the Pacific and the Atlantic cyclone centers are almost identical. The two plots also have very similar detailed regional characteristics in the northwestern Pacific, where a tongue of cyclone frequency maximum extends southward along the west coast of North America. In the Atlantic, maximum frequency bands in both plots exhibit a marked southwest–northeast orientation. The maximum cyclone frequency in the vicinity of the Mediterranean is also correctly reproduced by these criteria. Figure 2 is the same as Fig. 1 except for anticyclones. Compared with the cyclone centers in Fig. 1, the anticyclones occur at relatively lower latitude and their frequency bands extend more along latitudinal lines. In Fig. 2a, the orientation and geographic position of the two bands of maximum anticyclone frequency are very close to those in Fig. 2b. The three high-frequency centers at around 170°–180°E, 130°W, and 30°W agree well between the two plots. The high-frequency center near the Tibetan Plateau in Fig. 2b is a reflection of the Siberian high associated with the Asian winter monsoon. The area is not of major interest in this study and is therefore excluded from Fig. 2a.

In general, the geographic locations of the surface cyclone and anticyclone frequency identified through these criteria agree well with the respective results from Petterssen (1956), although a quantitative comparison between the two is very difficult. This is because the frequency of cyclones and anticyclones is computed in terms of the percentage of frequency of every 100 000 km^2 in Petterssen's study, while the frequency is measured in real numbers in the current study.

In order to quantitatively compare the current cyclone and anticyclone frequency distribution with those from the previous studies, we reconstructed Fig. 3, the northern winter seasonal mean (1958–77) cyclone frequency distribution based on the monthly data from Whittaker and Horn (1982). As expected, the qualitative features of Fig. 3 are very similar to those of Figs. 1a,b. Although there was a decrease in cyclone frequency from the 1950s to the 1970s in North America, it did not seem to affect the averaged geographic distribution of the cyclones. In a quantitative sense, the Pacific and the Atlantic maximum frequency in Fig. 3 is typically around 10 to 12 every season, while the magnitude of the same quantity is about 8 to 10 from Fig. 1a. In rough terms, the cyclone numbers in the Pacific, the Atlantic, and the Mediterranean from Fig. 1a are about two-thirds to approximately three-quarters of those from Fig. 3. The quantitative bias is very close to the cyclone frequency difference between the T42 and R15 resolution, as indicated by Giorgi (1990), which suggests that resolution is the major reason for the bias.

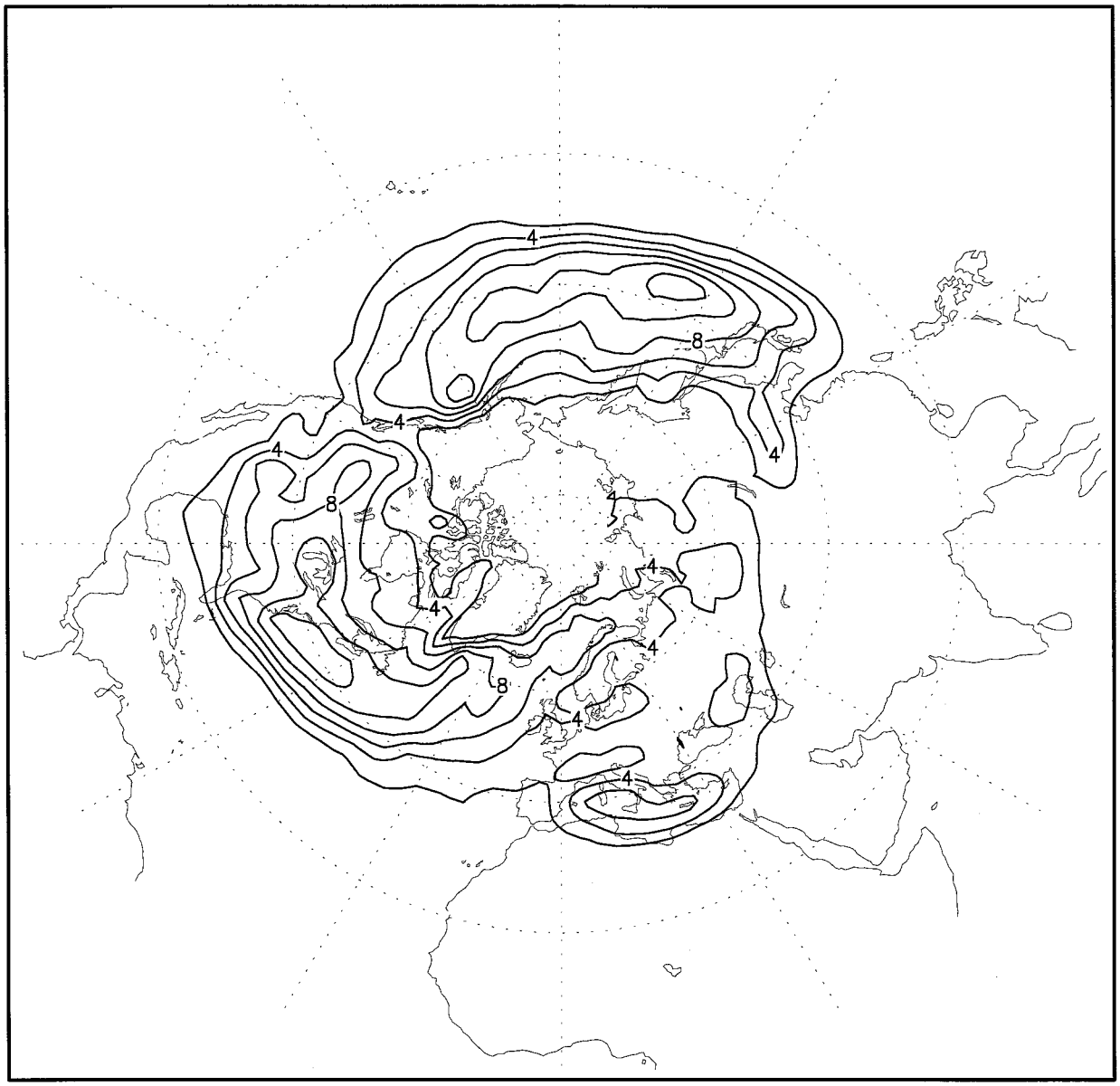

FIG. 3. Northern winter seasonal averaged (1958–77) cyclone frequency reconstructed from the data of Whittaker and Horn (1982). Contour interval is 2. Units are the numbers of events per season.

Despite this bias, the R15 data realistically reproduced the centers and geographic locations of cyclone and anticyclone frequency. Giorgi (1990) has also indicated that the R15 CCM1 can realistically portray the real geographic distribution and centers of maximum cyclone and anticyclone frequency.

4. Model results from warming and control simulations

a. Comparison between warming and control simulations

With the cyclone searching criteria tested, the previously mentioned variables can be used to analyze the cyclone and anticyclone activity under the greenhouse warming scenario.

Figure 4 shows cyclone frequencies from the control simulation and the difference (warming − control) of frequencies between the warming and the control simulations. Generally speaking, the two oceanic storm tracks and the center of maximum near the Mediterranean have been realistically reproduced. Although Fig. 4a consistently shows a lower magnitude of cyclone frequency than does Fig. 1a, the qualitative features are similar between the two, and Fig. 4a is quantitatively close to Fig. 1a. In the difference field, areas with both decreased and increased frequency can be found. The

magnitude and areas of decreased frequency clearly outnumber those of increased frequency. One particularly interesting phenomenon is that three of the most prominent minimum centers are found near the east coast of North America, east Asia and its surrounding oceans, and the Mediterranean. These three regions are among the most important cyclogenesis regions in the Northern Hemisphere (Petterssen 1956; Whittaker and Horn 1982). The decreases of the cyclone frequency in these regions suggest that the cyclongenesis has decreased.

Figure 5 is the same as Fig. 4 except for anticyclones. Compared with Fig. 2, the simulated anticyclone frequency is reasonably close to observations, although the maximum center near the eastern Atlantic is missing. In agreement with the change in cyclone frequency, the difference in anticyclone frequency shows a similar trend but exhibits a larger magnitude. The areas of decreased frequency clearly dominate over those of increased frequency. There is also decreasing near the east coast of the Pacific and over the entire Atlantic.

The eddy activity at 500 hPa can be studied by examining the bandpass filtered (period 2.5–6 days) rms value of 500-hPa geopotential height. Because surface cyclones and anticyclones are always associated with wave patterns in the middle to upper troposphere, high values of this quantity are expected near areas where cyclones and anticyclones often occur. Consistent with the trend at the surface, the eddy activity decreases at 500 hPa, as indicated in Fig. 6. The maximum reduction tends to occur over regions where cyclone-scale eddies are found to be most active, including the east coastal regions of North America and Asia and the mid-Atlantic. It should be mentioned that the dipole pattern near the Bering Strait is not a location where cyclones and anticyclones frequently occur, and it is therefore omitted from the discussion. The reduction over the two coastal regions is consistent with the trend of surface cyclones and anticyclones. A similar decreasing pattern in the standard deviation of 500-mb geopotential height was found by Bates and Meehl (1985) in a $2 \times CO_2$ simulation using an earlier version of the NCAR CCM. They have also found that the intensity of blocking did not change significantly, although the location moved geographically.

Figure 7 shows the 780-hPa Eady growth rate maximum from the control simulation and the difference between the warming and control simulations. This variable, also called the baroclinic parameter, can be represented in the form

$$\sigma_{BI} = 0.31 f \left| \frac{\partial V}{\partial Z} \right| N^{-1},$$

where 0.31 is a nondimensional coefficient, f is the Coriolis parameter, N is static stability, V is total wind, and Z is height. This parameter was first shown by Lindzen and Farrell (1980) to be an accurate estimate of the growth rate maximum in a range of baroclinic instability problems. Hoskins and Valdes (1990) used this parameter as a measure of the basic flow baroclinicity and indicated that a proper way to determine its value is to calculate it above the boundary layer where N tends not to play a dominant role. They also found that this quantity at 780 hPa coincided well with the 500-hPa storm tracks. The region in Fig. 7 where the 780-hPa level is within 1 km of the orography and probably in the boundary layer is blocked.

Comparing Fig. 7a with Fig. 6a, we noticed that, as expected, the two storm tracks at 500 hPa coincide with bands of a high baroclinicity parameter at 780 hPa. In the difference field, the general reduction of the atmospheric baroclinicity occurs in most areas of the midlatitudes. The magnitude of the decrease in these areas ranges from 0 to 0.08 day^{-1}.

If the mean baroclinicity and the Eady growth rate maximum are at all related to the extratropical baroclinic eddy activity, the reduction in its magnitude implies less active cyclone-scale eddies, which agrees with what has been discussed above.

b. Physical mechanisms

The analyses of the variables related to the extratropical cyclone-scale eddies in the previous section have consistently indicated that the eddy activity decreases under the greenhouse warming scenario. In this section, we discuss the physical mechanisms that are responsible for the decrease.

The difference in surface air temperature between the two simulations is plotted in Fig. 8. Note that the large magnitude of warming generally occurs at higher latitudes, which is a consistent feature of all models due to the feedback between temperature and snow–ice albedo (Mitchell et al. 1990). The nonuniform warming pattern means a weaker meridional surface air temperature gradient in the extratropical region. Because the baroclinicity of the flow and the strength of the cyclone-scale eddies are inherently related to the meridional temperature gradient throughout the troposphere, the reduction of the surface temperature gradient alone does not necessarily mean the weakening of the mean flow baroclinicity. Plotted in Fig. 9 is the zonally averaged vertical distribution of temperature difference between the two simulations. There is a very strong temperature increase north of 60°N and below 1 km, and a decreasing temperature gradient in the extratropics up to 5 km. Clearly, a reduction in the temperature gradient of such depth will weaken the atmospheric mean flow baroclinicity. A slight increase in the temperature gradient occurs above 5 km. This increase in the upper troposphere may slightly offset the effect of the decreasing temperature in the lower troposphere. But the vertical extent and magnitude of the increasing temperature gradient are not nearly as large and strong as those of the decreasing gradient. Also, even if the upper tropospheric effect is comparable to that of the lower troposphere, the sign of the lower-level temperature gradient would

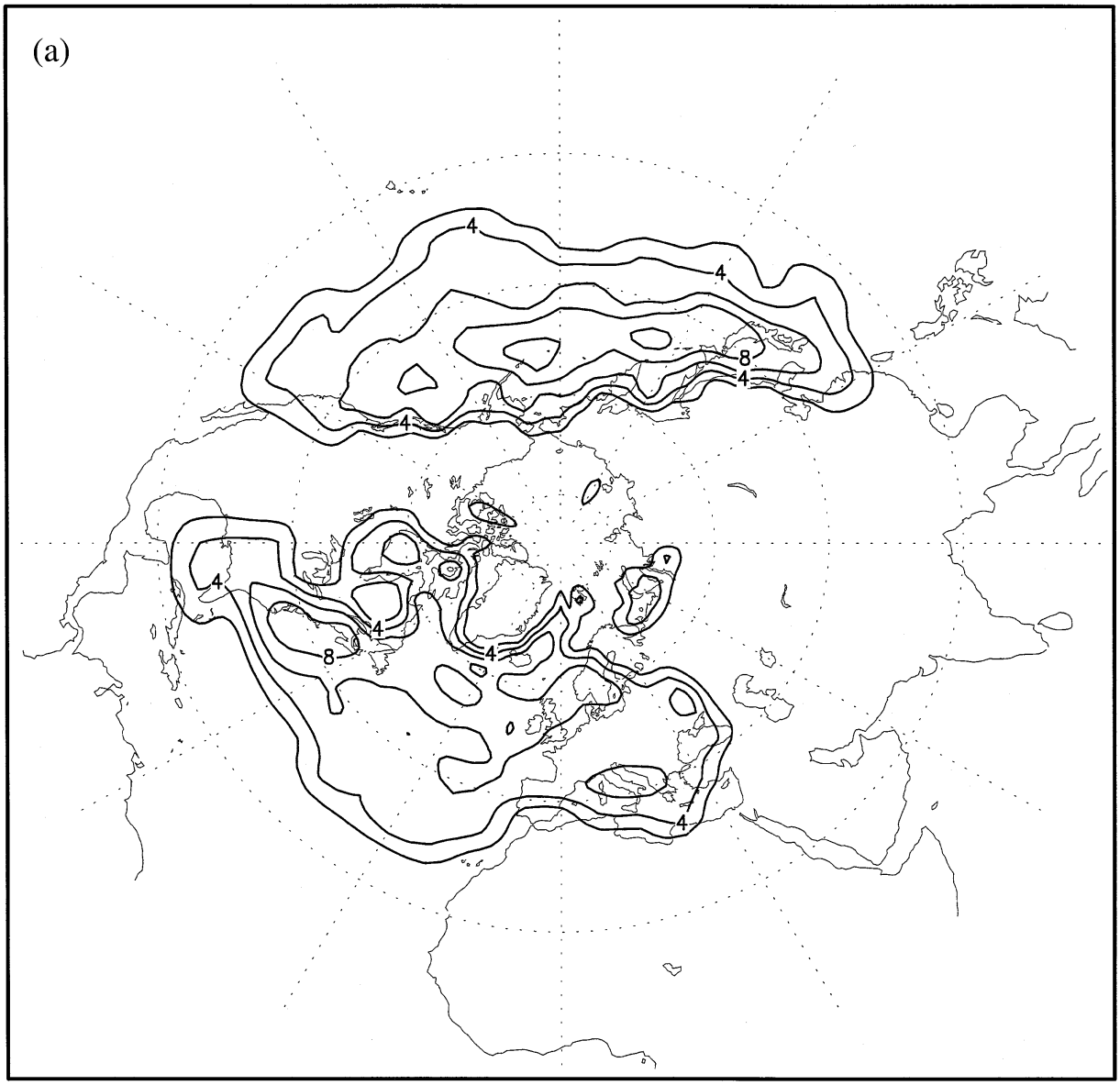

FIG. 4. (a) Winter seasonal averaged geographical distribution of cyclone frequency from the control simulation. Contour interval is 2. Units are the numbers of events per season. (b) Difference in cyclone frequency between warming and control simulations. Contour interval is 2. Units are the numbers of events per season.

likely still be dominant, as suggested by Held and O'Brien (1992), who show that the eddy heat flux is more sensitive to the lower-level than to the upper-level mean temperature gradient for equal values of vertical wind shear in an idealized quasigeostrophic model.

Another prominent feature from Fig. 8 is that the magnitude of warming over the continents is much larger than the warming over the oceans. As a result of this, the direct thermal contrast between the oceans and the continents is reduced, an effect considered by Sutcliffe (1951) to be a primary reason for the existence of the troughs to the east of the American and Asian continents. The direct thermal effect of the land and sea is of great significance to the differences between the summer and winter flow patterns near the east coasts of the two continents and the associated cyclone-scale disturbances downstream. The weakening of the thermal contrast will shift the coastal circulations toward their summer counterparts and thus tend to reduce the intensity of the troughs and the activity of the eddies.

On the other hand, the reduction in coastal thermal contrast also directly decreases the local baroclinicity in the coastal regions, which produces a less favorable condition for coastal frontogenesis, cyclongenesis, and development. Depending on the magnitude of the reduction in the coastal temperature gradient, the fre-

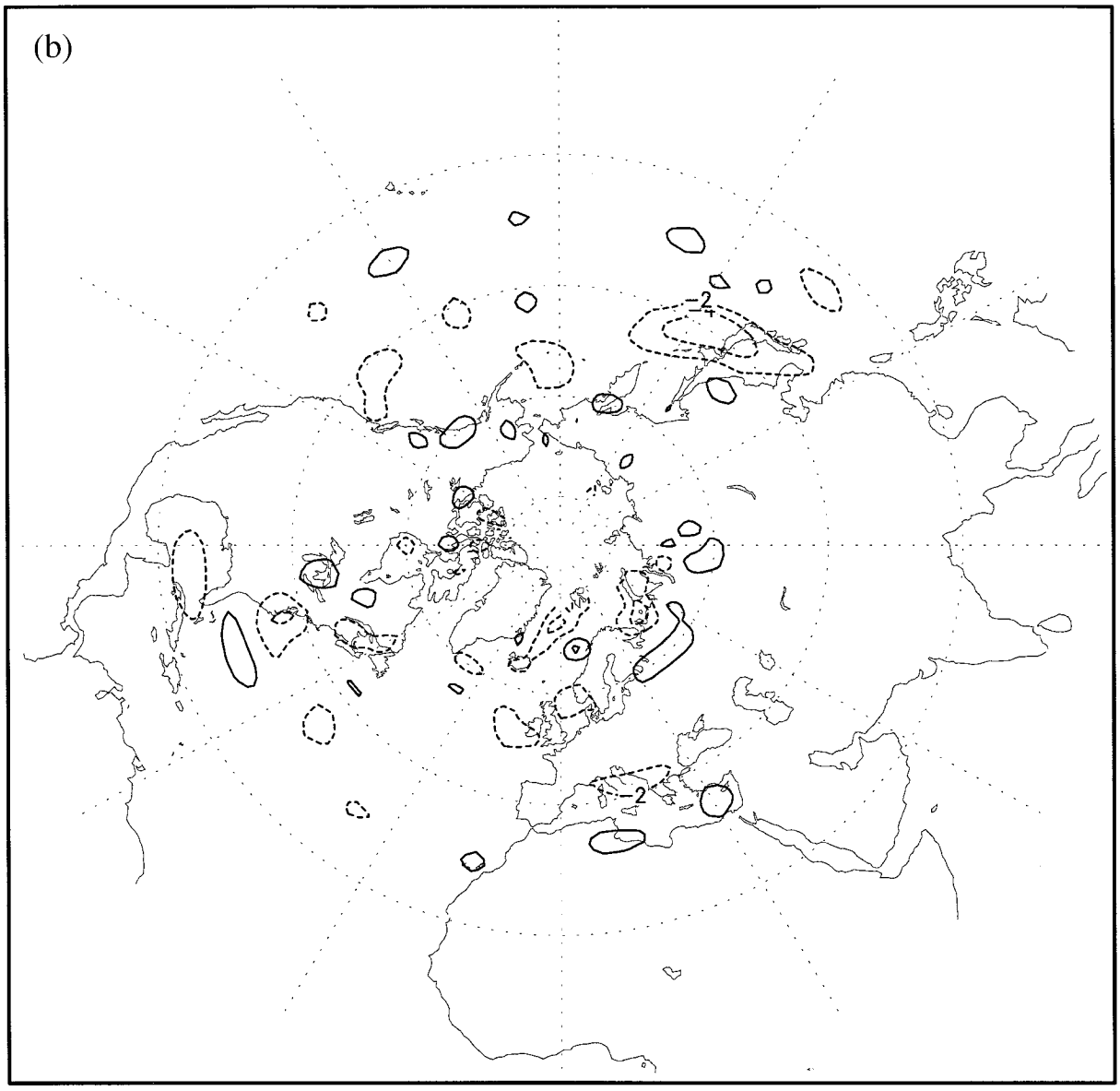

FIG. 4. (*Continued*)

quency of coastal cyclogenesis and the intensity of cyclone activity will possibly become lower and weaker. This is because, given the same upper-level vorticity advection, a weaker-than-normal low-level temperature gradient will be less likely to trigger the cyclongenesis. This type of cyclone development scenario in the coastal region of North America is referred to as ''type B'' by Petterssen (1956). A similar type of cyclone development was also found on the east coast of Asia (Chen et al. 1991). A likely result of this is that cyclones that would have formed under the normal condition will, in the warming case, either not form at all or will form with less intensity, depending on the reduction of the temperature gradient. This effect can greatly affect the total number and intensity of cyclone events because the east coastal regions of the two continents are the two major regions of cyclogenesis in the Northern Hemisphere (Petterssen 1956; Whittaker and Horn 1982). The reduction of cyclone numbers in the two major cyclongenesis regions in Fig. 4b suggests that this is what actually happened in the model simulation.

Another very important factor related to the eddy activity under the greenhouse warming scenario that has been suggested by Held (1993) is the global water vapor budget. Water vapor is the major absorber in the infrared contributing to the greenhouse effect. Its residence time in the atmosphere is on the order of a week and is controlled by convective, radiative, and dynamic processes

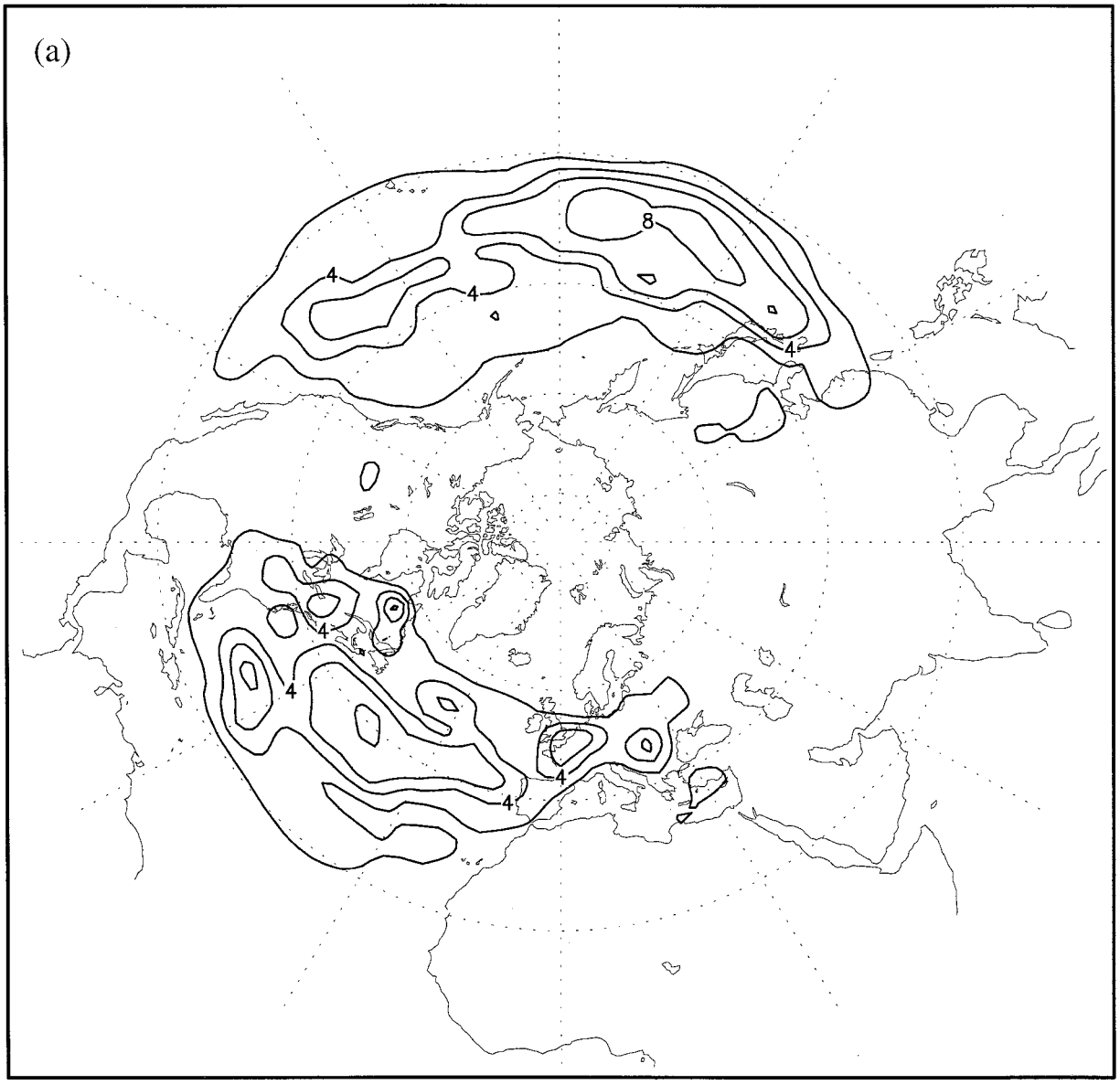

FIG. 5. (a) Winter seasonal averaged geographic distribution of anticyclone frequency from the control simulation. Contour interval is 2. Units are the numbers of events per season. (b) Difference of anticyclone frequency between warming and control simulations. Contour interval is 2. Units are the numbers of events per season.

in the atmosphere, and the changes in moisture content will affect the sources and sinks of latent heat, which will in turn affect the activity of cyclones and anticyclones (Danard 1964; Chen and Dell'Osso 1987).

The increase in specific humidity between the warming and control simulations, similar to those from Washington and Meehl (1984) and others, indicates that the maximum value is around 2 g kg^{-1} in the tropical to subtropical lower troposphere. The increase in moisture content is known to have the effect of enhancing the eddy activity. This is because the increase in moisture will increase the latent heat release in the warm sector of the baroclinic disturbance and, thus, enhance the transfer of available potential energy into kinetic energy as the warm air rises and moves poleward and the cold air sinks and moves equatorward. The increased moisture content will produce a more favorable environment for generating more kinetic energy and, thus, intensifying the eddy activity.

However, the increase in moisture content in the atmosphere has a different, but potentially more powerful, effect on the eddy activity. Since the increase in moisture content is more abundant in the low latitudes, the meridional eddy latent heat flux increases significantly under the warming condition. Plotted in Fig. 10 is the zonally averaged, vertically integrated eddy flux of the latent heat

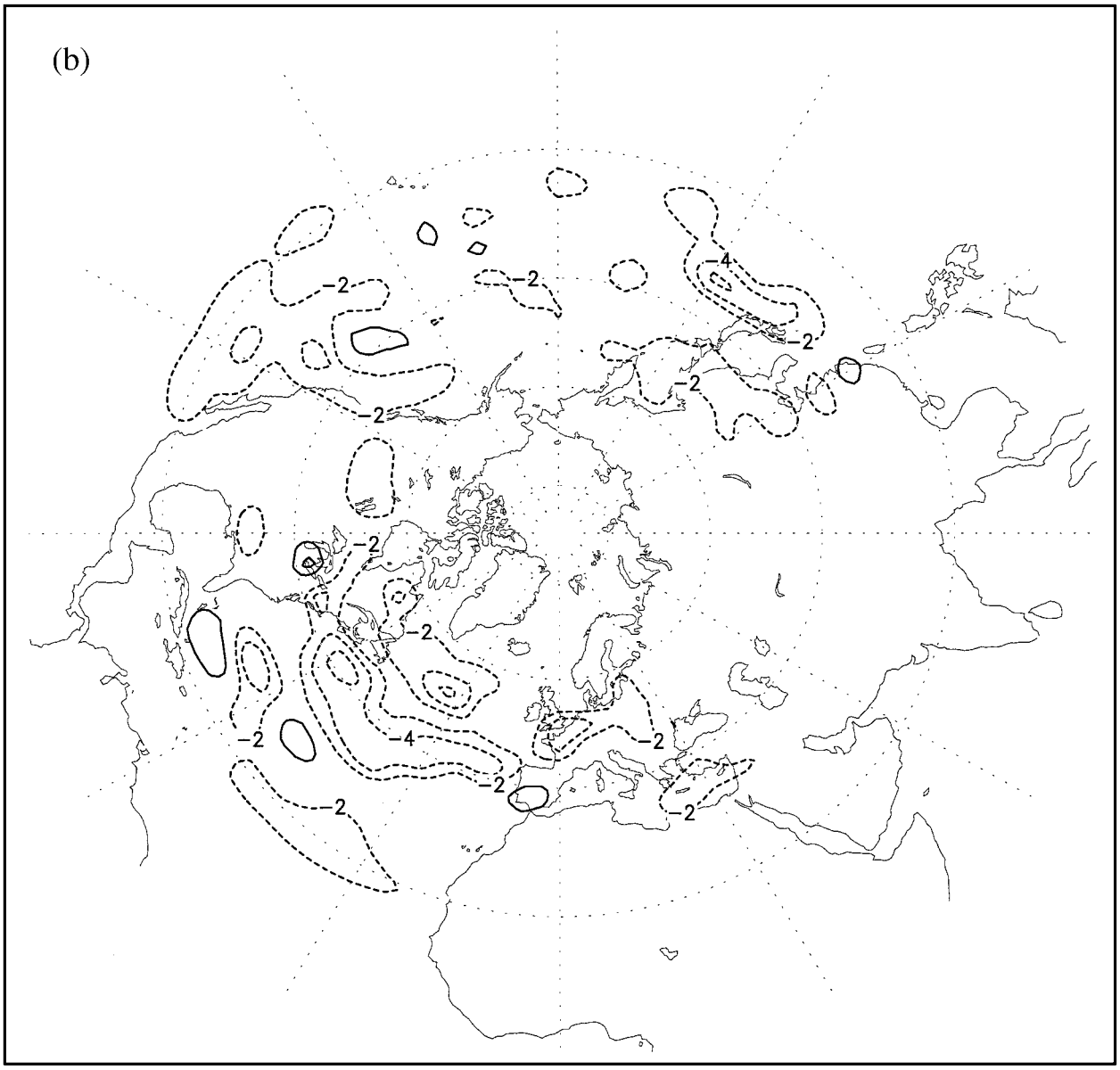

FIG. 5. (*Continued*)

of water vapor from both simulations. Although cyclone-scale eddies are less active in the warming condition, as indicated in the previous analysis, the eddy latent heat flux increases on average by about 0.4×10^{15} W around 30°–50°N. The part contributed by the cyclone-scale eddies (2.5–6 days) is about 0.2×10^{15} W. The reason for the increase is most likely due to the increase in moisture content under the warming condition, with more moisture in the subtropical air being transferred by the eddies to higher latitudes, where the temperature is relatively lower; the air thus becomes saturated, which results in more latent heat release. This is supported by the commonly known results regarding the increase in extratropical precipitation in warming conditions from many other GCMs (Mitchell et al. 1990) and this model.

As mentioned before, it is the balance between the equator-to-pole heating gradient and eddy heat flux that determines the meridional temperature gradient and the strength of the eddies. The increase in meridional eddy latent heat flux has two effects: first, it will reduce the meridional temperature gradient more than in the normal condition when less water vapor is transferred from the low latitudes; second, with the addition of more latent heat flux, the eddies become more efficient in transporting energy poleward. On a global average, fewer and less intense eddies are then required to maintain the

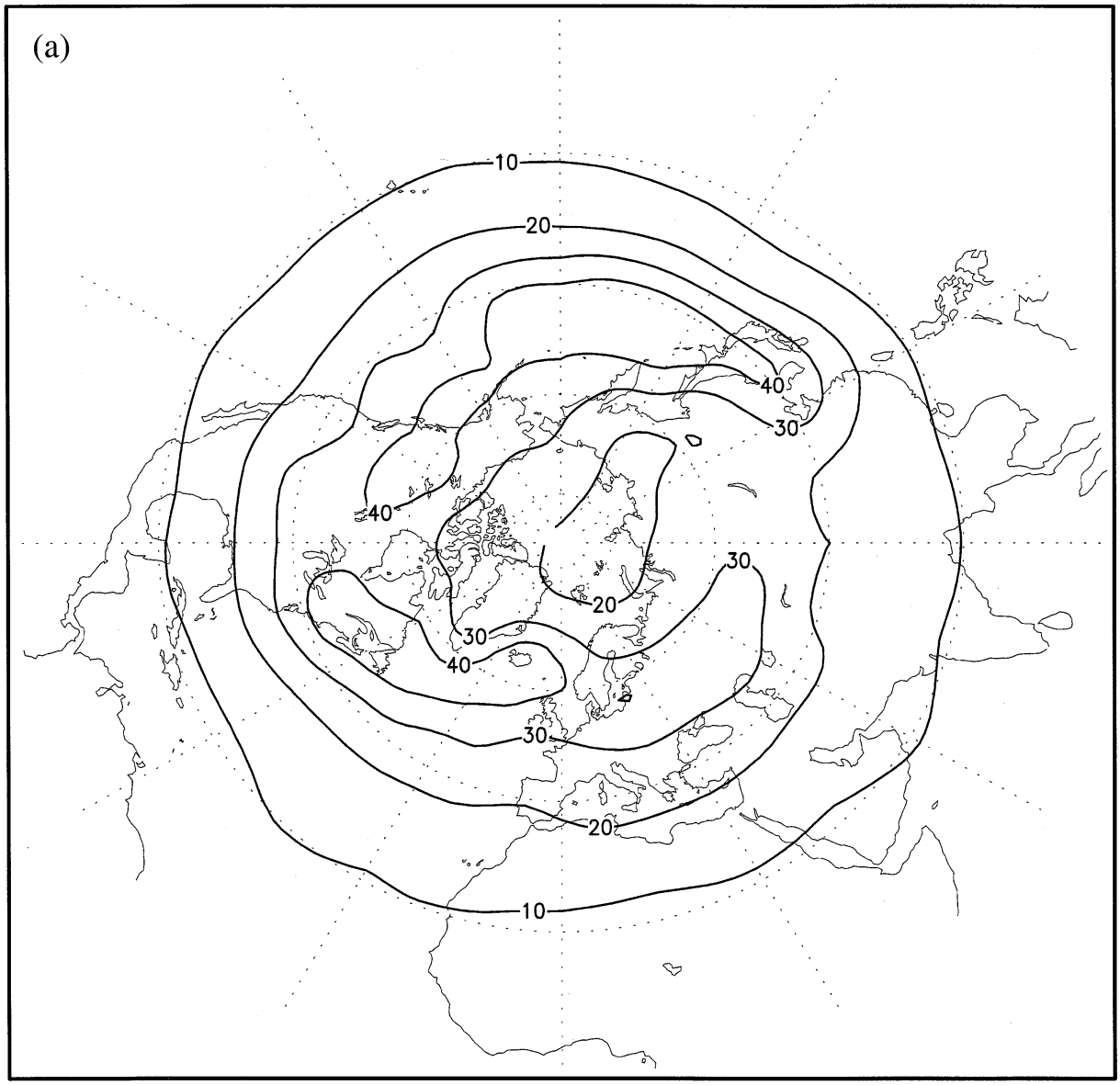

FIG. 6. (a) Winter seasonal averaged bandpassed rms of 500-hPa geopotential height from control simulation. Units are in meters. (b) Difference of rms of 500-hPa geopotential height at 4-m intervals between the warming and control simulations.

same (if not smaller) meridional temperature gradient. It is thus anticipated that the activity of cyclones and anticyclones will decrease as the moisture content increases under the warming condition.

Of the two opposing effects of the water vapor on the cyclone-scale eddy activity, the former is more important for mesoscale and small-scale disturbances. This is because moist dynamics tend to influence small-scale phenomena much more than the large-scale ones (Sardie and Warner 1983). On a planetary scale, the cyclone-scale eddies will be more affected by the latter. Therefore, we believe that the increase in moisture content will weaken the extratropical eddy activity.

5. Conclusions and discussion

The objectives of this study, as stated in the introduction, are to investigate the possible changes of cyclone and anticyclone activity under a greenhouse warming scenario. The following conclusions are reached.

1) The analysis of model-simulated variables has indicated that the cyclone and anticyclone activity mostly decreases under the greenhouse warming scenario. This decrease is not only reflected in the surface cyclone and anticyclone frequency and the bandpassed rms of 500-hPa geopotential height, but is also discernible from the Eady growth rate maximum.

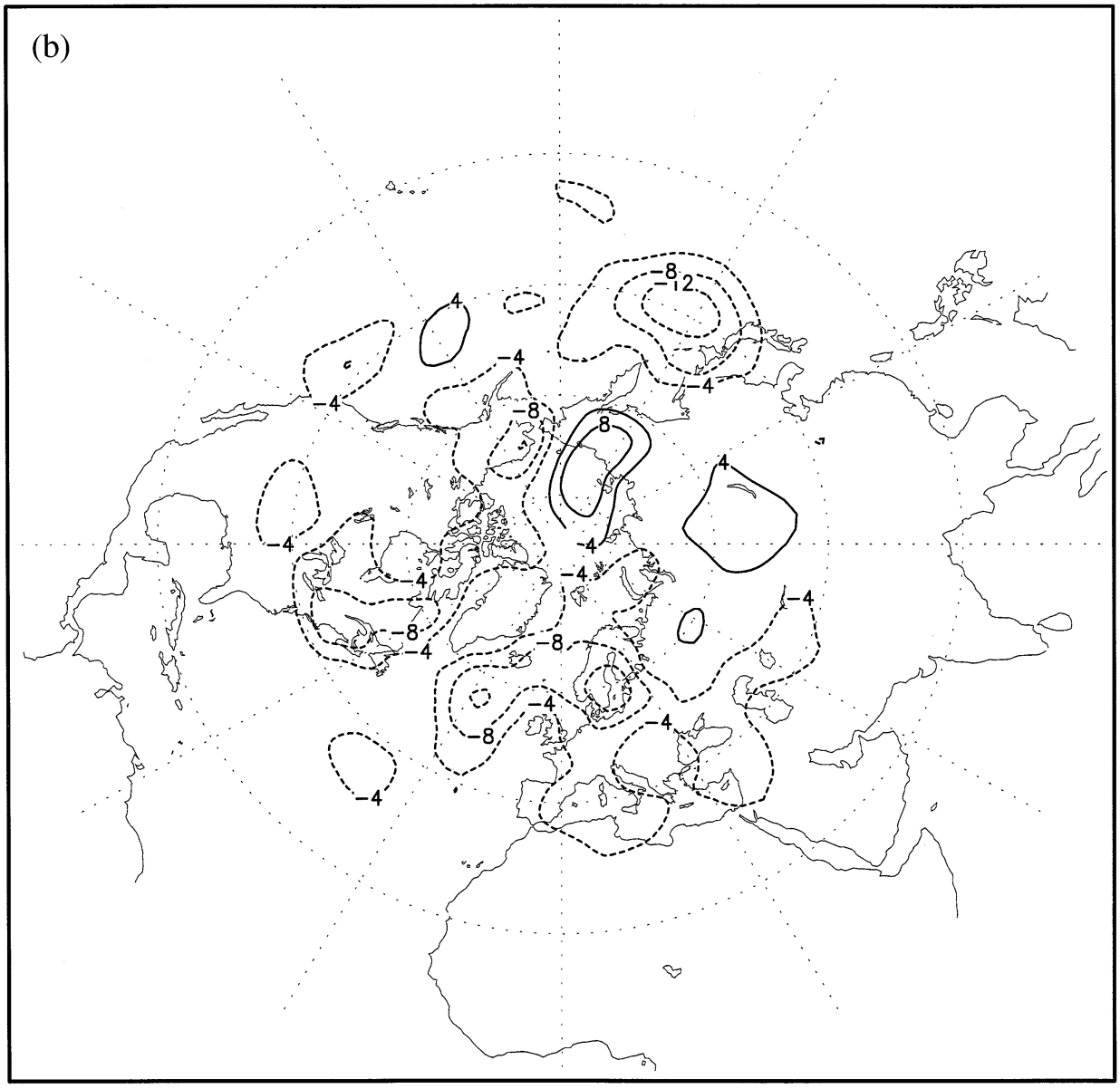

FIG. 6. (*Continued*)

2) Three different physical mechanisms contributed to the decreasing eddy activity: (a) the decrease of the extratropical lower- to midtropospheric meridional temperature gradient, (b) the reduction of the land–sea thermal contrast in the east coastal regions of the continents, and (c) the increase in eddy meridional latent heat fluxes.

Although this study indicates that cyclone-scale eddies become less active in a greenhouse warming climate in NCAR CCM1, the current analysis is far from complete, and further studies are warranted.

First, a complete and satisfactory discussion of the physical mechanisms that caused the decrease of eddy activity under the warming condition would not be achieved without the examination of the effect of the Hadley circulation, given that a change in the tropical heating structure could change the intensity of the Hadley circulation and thus may greatly affect the subtropical jet and the extratropical baroclinic wave activity (Chang 1995). According to Lindzen (1990), the mass flux in the tropical convective clouds increases with warming, and the increase in the mass flux will intensify the strength of the rising branch of the Hadley cell. If this is true, the subtropical high will be intensified, along with the baroclinicity and the subtropical jet stream. Depending on the magnitude of the intensification, the

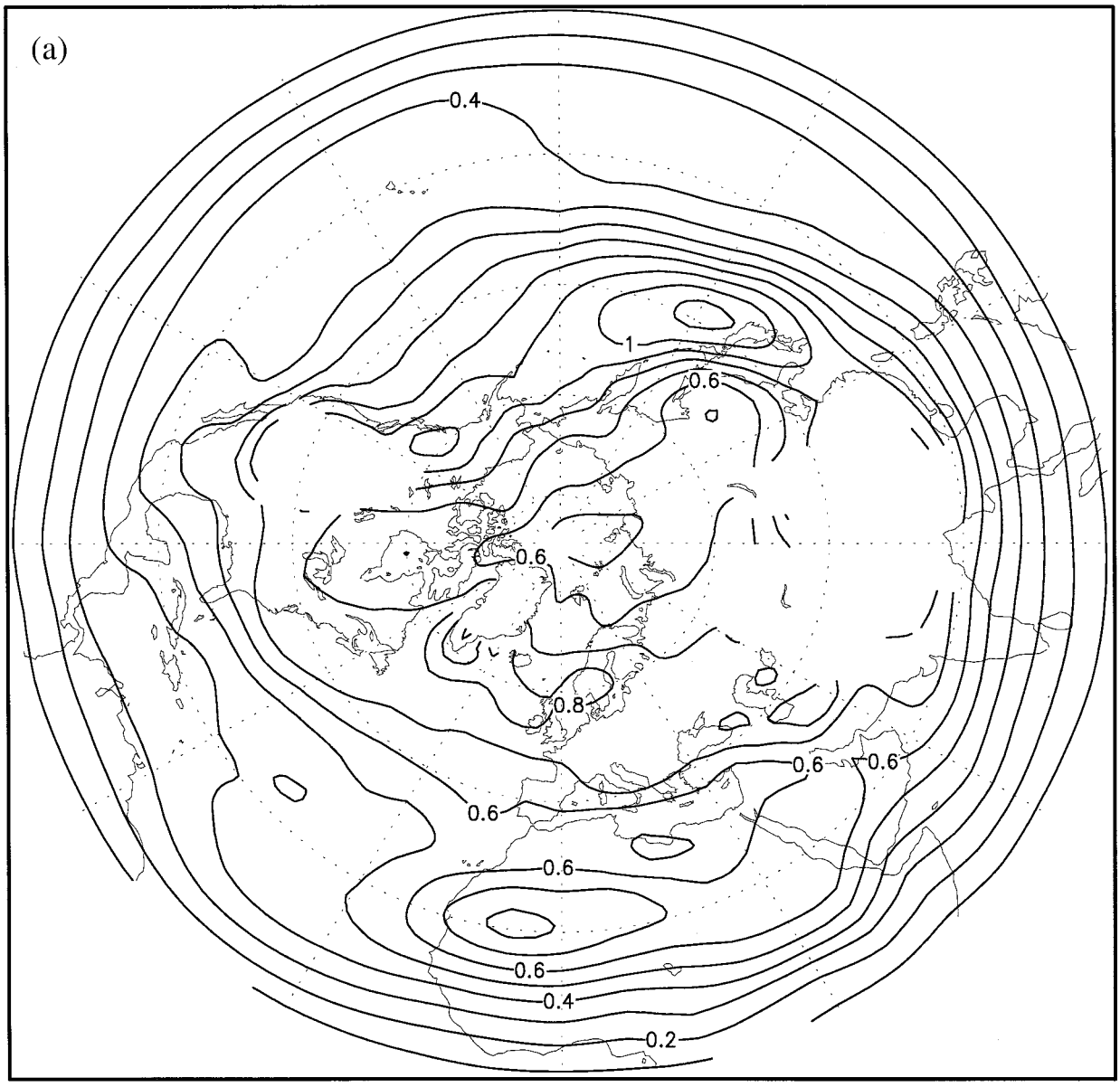

FIG. 7. (a) Winter seasonal averaged Eady growth rate maximum at 780 hPa from the control simulation at 0.1-day^{-1} intervals. (b) Difference of the Eady growth rate maximum between the warming and control simulations. Contour interval is 0.08. Units are in day^{-1}.

effect of the Hadley cell on the eddies could partly offset the effect of decreasing eddy activity.

The mean meridional streamfunction from the control and warming simulations was computed, and the maximum magnitude at the center of the Hadley cell was found to decrease by 16×10^9 kg s^{-1} (less than 10%) under the warming scenario. Del Genio et al. (1991) have indicated that the strength of the Hadley cell increases or decreases slightly depending on the version of the National Aeronautics and Space Administration/Goddard Institute of Space Sciences (NASA/GISS) model used. The most updated version of the NASA/GISS GCM shows a slight decrease in the Hadley cell intensity (A. Del Genio 1995, personal communication). Based on the results of the current model and those of the NASA/GISS model, the change in the intensity of the Hadley cell under the greenhouse warming scenario seems too small to have any significant effect on the extratropical cyclones and anticyclones. Clearly, this is a problem that needs to be further investigated.

Second, we must bear in mind that all our results are based on model equilibrium simulations. In reality, the concentration of greenhouse gases increases gradually and the climate responds slowly to the gradual changes of greenhouse gas concentrations. The thermal capacity of the oceans will delay and effectively reduce the cli-

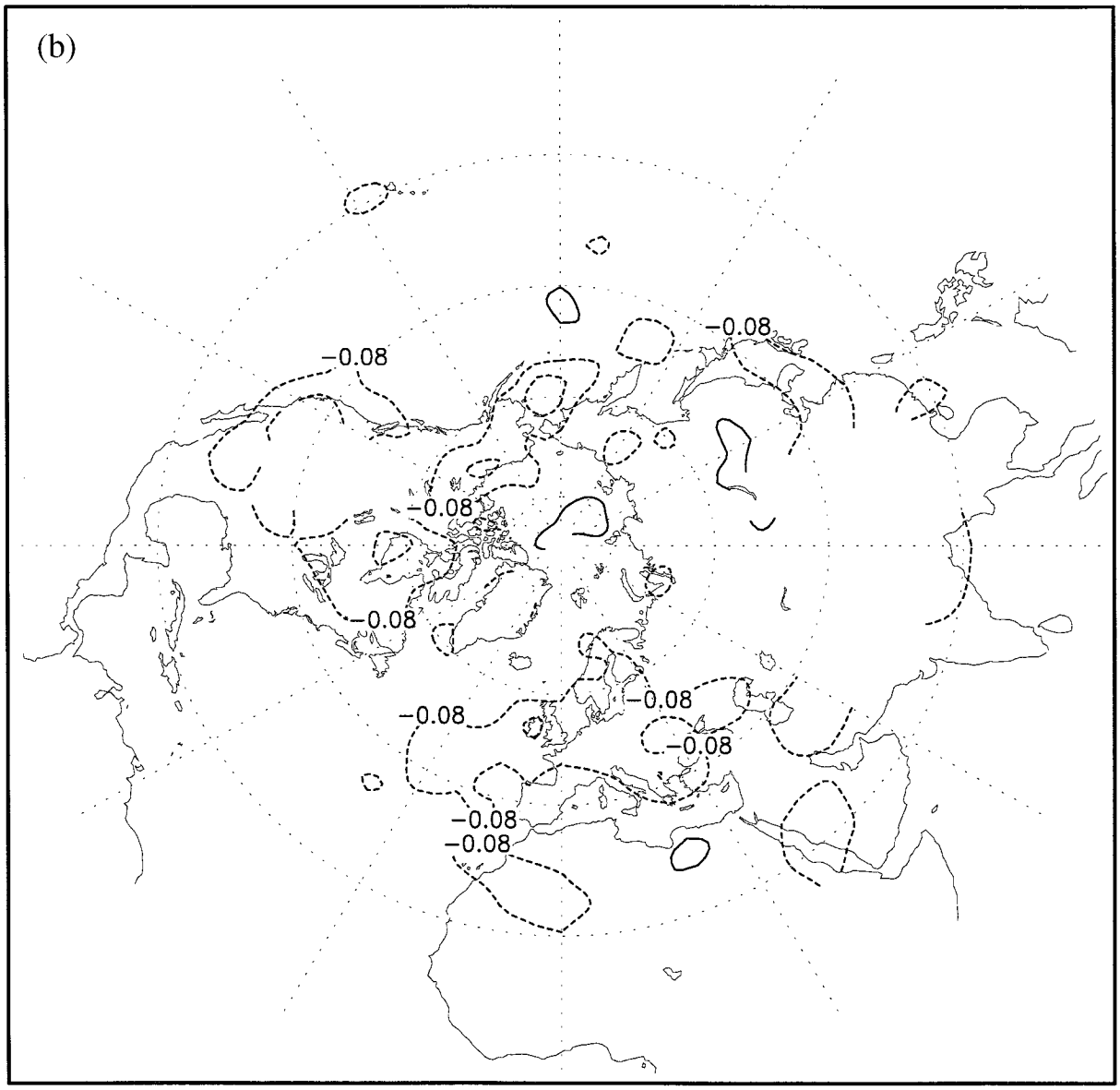

FIG. 7. (*Continued*)

matic response to the increased greenhouse gases. To make reliable predictions of climate change under realistic scenarios of increasing forcing by the increase of greenhouse gases, coupled atmosphere–ocean general circulation models are essential. Due to the computational constraint, only a few groups of researchers (Stouffer et al. 1989; Washington and Meehl 1989; Mitchell et al. 1995; Hasselmann et al. 1995) have performed transient simulations using fully coupled ocean–atmospheric models. The planetary response patterns for both temperature and precipitation of these coupled ocean–atmosphere models for a steadily increasing forcing generally resemble those of an equilibrium simulation, except that the increases are generally reduced in magnitude (Gates et al. 1992). One exception, however, is that the warming is reduced and delayed in the North Atlantic due to the deep mixing in the ocean model. This would, undoubtedly, complicate the processes of cyclongenesis in that region. However, it seems that if the warming is reduced in the ocean, the land–ocean thermal contrast will be further decreased as compared to that of the mixed-layer simulations. Physical mechanisms discussed in the last section will still be valid for the coupled ocean–atmosphere simulations. Taking this into consideration, the present conclusions concerning the changing eddy activity will be affected quantitatively, not qualitatively. Therefore, there still will be fewer active extratropical cyclone-

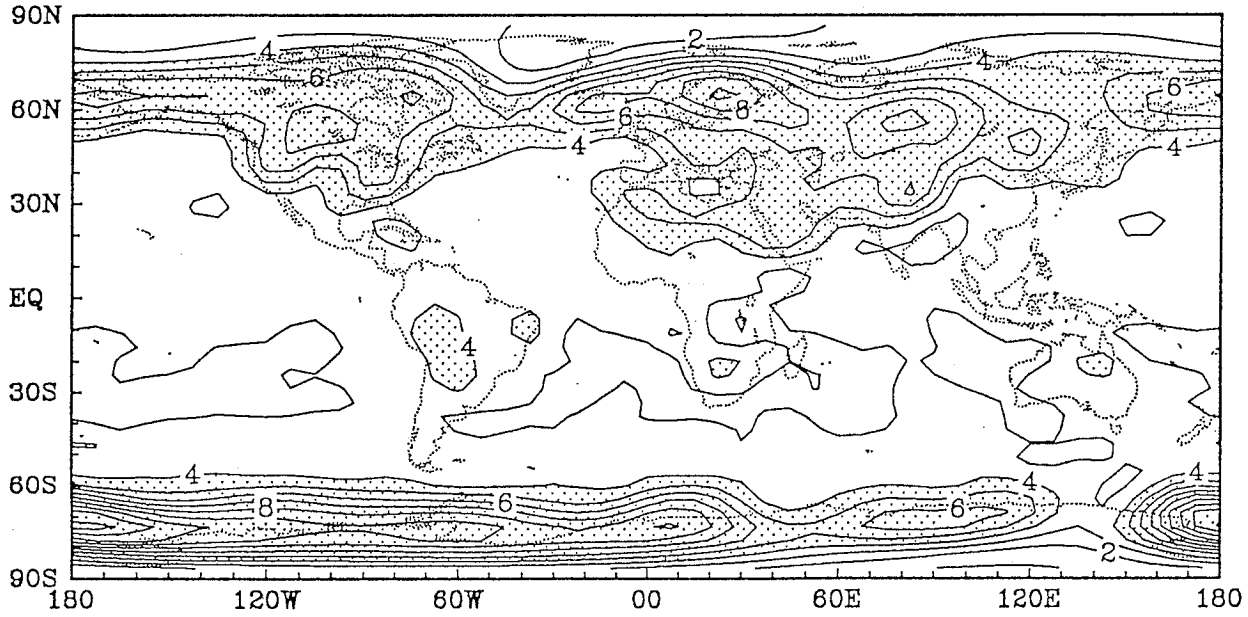

FIG. 8. Difference of the winter seasonal averaged surface air temperature between warming and control simulations. Contour interval is 1.0°C. Areas with warming greater than 4°C are shaded.

scale eddies under the greenhouse warming scenario, but the magnitude of the decrease will likely be less than that estimated from the equilibrium simulations.

Finally, all the results discussed here are based on simulations from one model. In general, the model-simulated results from the control or the perturbed runs are a combination of real climate change, which is physically caused and changes due to errors that are inherently re-

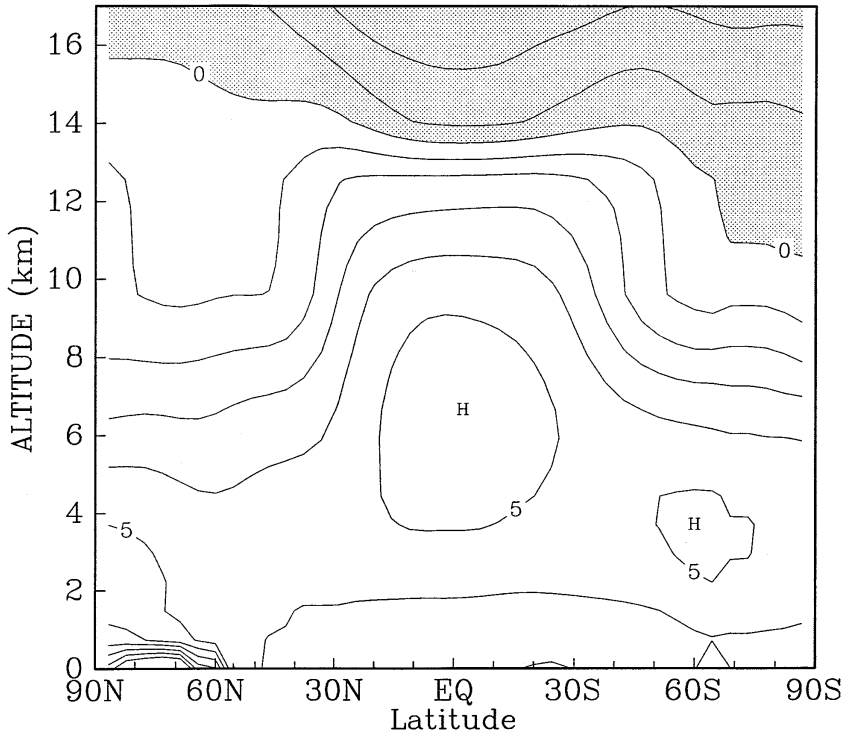

FIG. 9. Zonal mean vertical distribution of temperature difference between warming and control simulations at 1.0°C intervals.

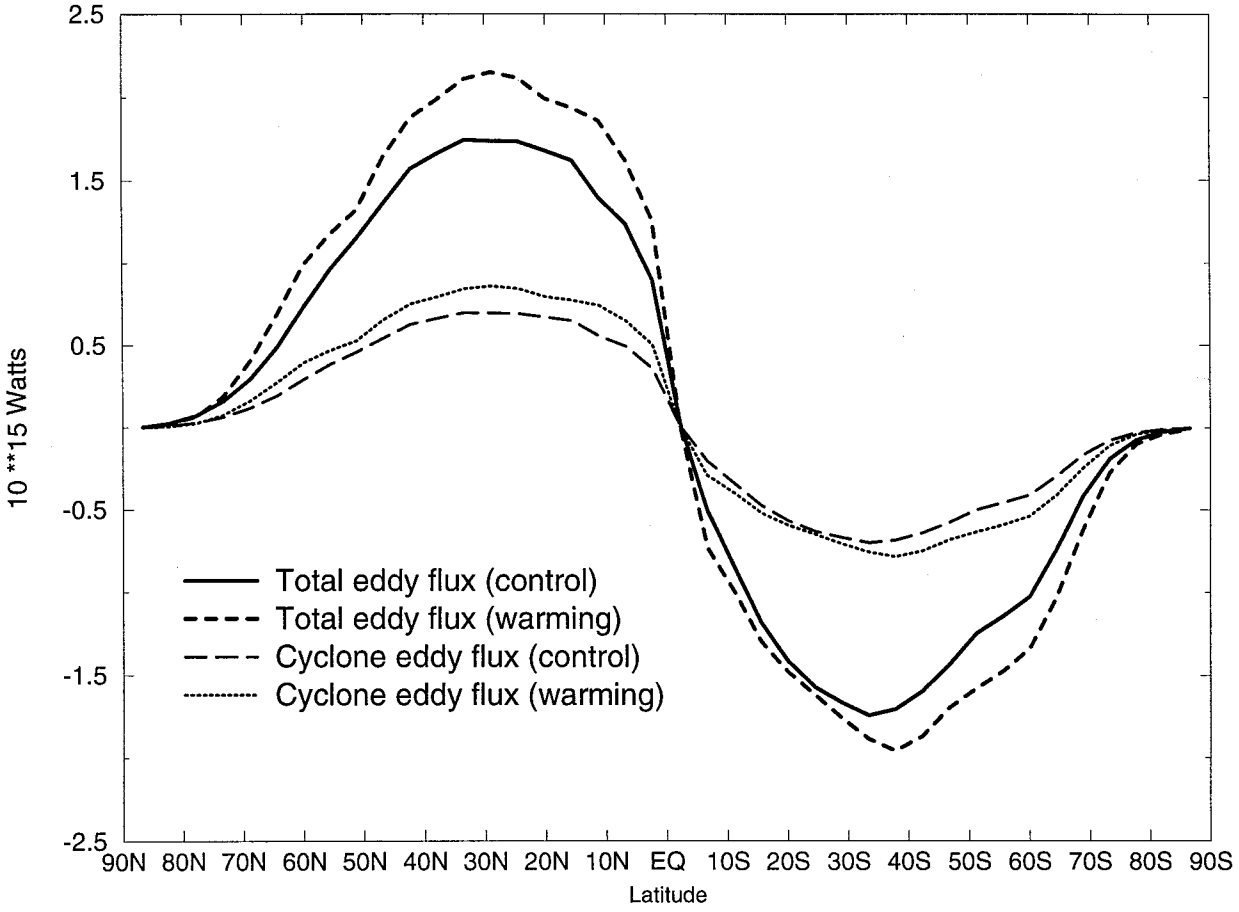

FIG. 10. Winter seasonal averaged northward mean meridional eddy flux of latent heat from the control and warming simulations. Units are in 10^{15} W.

lated to a specific model. The model-dependent uncertainties must be smaller than the real climate change if the model result is to be given credibility. It is very difficult to distinguish the real changes and model-dependent uncertainties in a quantitative way. The response of model results to a perturbation has been shown to depend on the control climate (Mitchell et al. 1987). Before the model is used to study this problem, the variables related to the cyclone-scale eddies from the control simulation have been thoroughly evaluated against observations (Zhang 1995). These model-simulated variables, which include surface cyclones and anticyclones and the bandpassed rms of 500-hPa geopotential height, are in general agreement with the observations.

However, a model indicating a good control simulation is not sufficient to guarantee that the perturbed runs will be equally well simulated unless the relevant physical mechanisms can be identified. During this study, the physical mechanisms related to the changing eddy activity have been discussed, and the physical interpretations are consistent with results that were derived from the model variables. We thus conclude, based on the results from the current model, that the northern winter extratropical cyclones and anticyclones will become less active in a global warming scenario.

Acknowledgments. This paper is based on a portion of the first author's Ph.D. thesis, completed under the second author's supervision at the State University of New York at Albany. We are indebted to W. Lawrence Gates for his invaluable suggestions and a thorough review of an earlier draft. Comments and suggestions from James S. Boyle, Kenneth R. Sperber, and two anonymous reviewers are greatly appreciated. James S. Boyle also provided the data for Fig. 3. We wish to thank Anthony D. Del Genio for sharing some results from the NASA/GISS model and constructive discussions. Michael Fiorino and Anna McCravy helped with some of the figures. This work was supported by the Environmental Science Division of the U.S. Department of Energy under Contracts DEFG-0292-ER-61369 and W-7405-ENG-48, and the Climate Dynamics Division of the National Science Foundation under Contract ATM-9415336.

REFERENCES

Bates, G. T., and G. A. Meehl, 1986: The effects of CO_2 concentration on the frequency of blocking in a general circulation model coupled to a simple mixed layer ocean model. *Mon. Wea. Rev.,* **114,** 687–701.

Chang, E. K. M., 1995: The influence of Hadley circulation intensity changes on extratropical climate in an idealized model. *J. Atmos. Sci.,* **52,** 2006–2024.

Chen, S.-J., and L. Dell'Osso, 1987: A numerical case study of east Asian coastal cyclogenesis. *Mon. Wea. Rev.,* **115,** 477–487.

——, Y.-H. Kuo, P.-Z. Zhang, and Q.-F. Bai, 1991: Synoptic climatology of cyclogenesis over east Asia, 1958–1987. *Mon. Wea. Rev.,* **119,** 1407–1418.

Covey, C., and S. T. Thompson, 1989: Testing the effects of ocean heat transport on climate. *Palaeogeogr. Palaeoclimatol. Palaeoecol.,* **75,** 331–341.

Darnard, M. B., 1964: On the influence of released latent heat on cyclone development. *J. Appl. Meteor,* **3,** 27–37.

Del Genio, A. D., A. A. Lacis, and R. A. Ruedy, 1991: Simulations of the effect of a warmer climate on atmospheric humidity. *Nature,* **351,** 382–385.

Gates, W. L., J. F. B. Mitchell, G. J. Boer, U. Cubasch, and V. P. Meleshko, 1992: Climate modeling, climate prediction and model validation. *Climate Change 1992, The Supplementary Report to the IPCC Scientific Assessment,* J. T. Houghton, B. A. Callander, and S. K. Varney, Eds., Cambridge University Press, 101–129.

Giorgi, F., 1990: Simulation of regional climate using a limited area model nested in a general circulation model. *J. Climate,* **3,** 941–963.

Hall, N. M. J., B. J. Hoskins, P. J. Valdes, and C. A. Senior, 1994: Storm tracks in a high-resolution GCM with doubled carbon dioxide. *Quart. J. Roy. Meteor. Soc.,* **120,** 1209–1230.

Hasselmann, K., and Coauthors, 1995: Detection of anthropogenic climate changes using a fingerprint method. MPI Rep. 168, 20 pp. [Available from Max-Planck-Institut für Meteorologie, Hamburg D-20146, Germany.]

Held, I. M., 1993: Large-scale dynamics and global warming. *Bull. Amer. Meteor. Soc.,* **74,** 228–241.

——, and E. O'Brien, 1992: Quasigeostrophic turbulence in a three-layer model: Effects of vertical structure in the mean shear. *J. Atmos. Sci.,* **49,** 1861–1870.

Holopainen, E. O., 1965: On the role of mean meridional circulations in the energy balance of the atmosphere. *Tellus,* **17,** 285–294.

Hoskins, B. J., and P. J. Valdes, 1990: On the existence of storm-tracks. *J. Atmos. Sci.,* **47,** 1854–1864.

Houghton, J. T., G. J. Jenkins, and J. J. Ephraums, Eds., 1990: *Climate Change, The IPCC Scientific Assessment.* Cambridge University Press, 364 pp.

——, B. A. Callander, and S. K. Varney, Eds., 1992: *Climate Change 1992, The Supplementary Report to the IPCC Scientific Assessment.* Cambridge University Press, 200 pp.

——, L. G. Meira Filho, J. Bruce, H. S. Lee, B. A. Callander, E. Haites, N. Harris, and K. Maskell, 1995: *Climate Change 1995,* Cambridge University Press, 572 pp.

Kiehl, J., and D. Williamson, 1991: Dependence of cloud amount on horizontal resolution in the National Center for Atmospheric Research Community Climate Model. *J. Geophys. Res.,* **96,** 10 955–10 980.

Klein, W. H., 1957: The frequency of cyclones and anticyclones in relation to the mean circulation. *J. Meteor.,* **15,** 98–102.

Konig, W., R. Sausen, and F. Sielmann, 1993: Objective identification of cyclones in GCM simulations. *J. Climate,* **6,** 2217–2231.

Lambert, S. J., 1988: A cyclone climatology of the Canadian Climate Centre general circulation model. *J. Climate,* **1,** 109–115.

——, 1995: The effect of enhanced greenhouse warming on winter cyclone frequencies and strengths. *J. Climate,* **8,** 1447–1452.

Lindzen, R. S., 1990: Some coolness concerning global warming. *Bull. Amer. Meteor. Soc.,* **71,** 288–299.

——, and B. Farrell, 1980: A simple approximate result for the maximum growth rate of baroclinic instabilities. *J. Atmos. Sci.,* **37,** 1648–1654.

Mitchell, J. B., C. A. Wilson, and W. M. Cunnington, 1987: On CO_2 climate sensitivity and model dependence of results. *Quart. J. Roy. Meteor. Soc.,* **113,** 293–322.

——, S. Manabe, T. Tokioka, and V. Meleshko, 1990: Equilibrium climate change. *Climate Change, The IPCC Scientific Assessment,* J. T. Houghton, G. J. Jenkins, and J. J. Ephraums, Eds., Cambridge University Press, 131–176.

——, T. C. Johns, J. M. Gregory, and S. F. B. Tett, 1995: Climate response to increasing levels of greenhouse gases and sulphate aerosols. *Nature,* **376,** 501–504.

Newton, C., 1969: The role of extratropical disturbances in the global atmosphere. *The Global Circulation of the Atmosphere,* Royal Meteorological Society, 137–158.

——, and E. O. Holopainen, 1990: *Extratropical Cyclones: The Erik Palmen Memorial Volume.* Amer. Meteor. Soc., 262 pp.

Petterssen, S., 1956: *Weather Analysis and Forecasting.* 2d ed. Vol. 1, McGraw-Hill, 422 pp.

Sardia, J. M., and T. T. Warner, 1983: On the mechanism for the development of polar lows. *J. Atmos. Sci.,* **40,** 869–881.

Stouffer, R. J., S. Manabe, and K. Bryan, 1989: Interhemispheric asymmetry in climate response to a gradual increase of atmospheric carbon dioxide. *Nature,* **342,** 660–662.

Sutcliffe, R. C., 1951: Mean upper contour patterns of the Northern Hemisphere—The thermal-synoptic viewpoint. *Quart. J. Roy. Meteor. Soc.,* **77,** 435–440.

Trenberth, K. E., 1991: Storm tracks in the Southern Hemisphere. *J. Atmos. Sci.,* **48,** 2159–2178.

Wang, W.-C., M. P. Dudek, X.-Z. Liang, and J. T. Kiehl, 1991: Inadequacy of effective CO_2 as a proxy in simulating the greenhouse effect of other radiatively active gases. *Nature,* **350,** 573–577.

——, ——, and ——, 1992: Inadequacy of effective CO_2 as a proxy in assessing the regional climate change due to other radiatively active gases. *Geophys. Res. Lett.,* **19,** 1375–1378.

Washington, W. M., and G. A. Meehl, 1984: Seasonal cycle experiment on the climate sensitivity due to a doubling of CO_2 with an atmospheric general circulation model coupled to a simple mixed-layer ocean model. *J. Geophys. Res.,* **89,** 9475–9503.

——, and ——, 1989: Climate sensitivity due to increased CO_2: Experiments with a coupled atmosphere and ocean general circulation model. *Climate Dyn.,* **4,** 1–38.

Whittaker, L. M., and L. H. Horn, 1981: Geographical and seasonal distribution of North America cyclogenesis 1958–1977. *Mon Wea. Rev.,* **109,** 2312–2322.

——, and ——, 1982: Atlas of Northern Hemisphere extratropical cyclone activity, 1958–1977. Res. Rep., 40 pp. [Available from University of Wisconsin—Madison, Madison, WI 53706.]

Williamson, D. L., J. T. Kiehl, V. Ramanathan, R. E. Dickinson, and J. Hack, 1987: Description of NCAR Community Climate Model (CCM1). NCAR Tech. Note NCAR/TN-285+STR, 112 pp. [Available from NCAR Scientific Division, National Center for Atmospheric Research, Boulder, CO 80307.]

Williamson, G. S., and D. L. Williamson, 1987: Circulation statistics from seasonal and perpetual January and July simulations with the NCAR Community Climate Model (CCM1):R15. NCAR Tech. Note NCAR/TN-258+STR, 199 pp. [Available from NCAR Scientific Division, National Center for Atmospheric Research, Boulder, CO 80307.]

Zhang, Y., 1995: Extratropical cyclone-scale eddies simulated from a climate model. Ph.D. dissertation, State University of New York at Albany, 161 pp. [Available from University Microfilm, 1400 Washington Avenue, Albany, NY 12222.]

Zishka, K. M., and P. J. Smith, 1980: The climatology of cyclones and anticyclones over North America and surrounding ocean environs for January and July, 1950–77. *Mon. Wea. Rev.,* **108,** 387–401.